Nucl. Phys. B 1003 (2024) 116465

Contents lists available at ScienceDirect

Nuclear Physics, Section B

journal homepage: www.elsevier.com/locate/nuclphysb

High Energy Physics – Phenomenology

Transition Edge Sensors with Sub-eV Resolution And Cryogenic Targets (TESSERACT) at the underground laboratory of Modane (LSM)

J. Billard [a,*], J. Gascon [a], S. Marnieros [b], S. Scorza [c]

[a] Univ Lyon, Université Lyon 1, CNRS-IN2P3, IP2I-Lyon, Villeurbanne, F-69622, France
[b] Université Paris-Saclay, CNRS-IN2P3, IJCLab, Orsay, 91405, France
[c] Univ. Grenoble Alpes, CNRS, Grenoble INP, LPSC-IN2P3, Grenoble, 38000, France

ARTICLE INFO

Editor: Tommy Ohlsson

ABSTRACT

The future TESSERACT experiment will search for individual galactic DM particles below the proton mass through interactions with advanced, ultra-sensitive detectors. Currently TESSERACT is in a design phase aiming to produce fully defined detector technologies that will explore DM masses down to 10 MeV. It is designed to be sensitive to DM candidates interacting with the detector target material in producing both nuclear recoil DM (NRDM) and electron recoil (ERDM). To do so, multiple target materials will be used with varying detection strategies to ensure the capability to both actively reject the so-called low-energy excess and discriminate nuclear recoils against electron recoils. In addition to maximizing sensitivity to a variety of DM interactions, this provides an independent handle on instrumental backgrounds. Nowadays, the TESSERACT project encompasses two US-based technologies, namely HeRALD using superfluid helium as a target material, and SPICE using polar crystals (Al_2O_3 and SiO_2) and scintillating crystals such as GaAs. In these proceedings, we discuss the recent proposal to host the future TESSERACT experiment at the Modane Underground Laboratory (LSM) and add a third French-based cryogenic semiconducting (Ge, Si) detector technology to the TESSERACT payload.

1. Searching for light dark matter with TESSERACT

1.1. Scientific motivations

Elucidating the identity of dark matter (DM) is one of the most compelling problems of high energy physics. For decades, theoretical and experimental probes have been focused on the weak scale in the search for answers to nature's deepest mysteries, including the identity of DM. This is understandable: in addition to connecting the DM problem to the question of the natural mass scale for the Higgs boson, the DM relic abundance falls out naturally from the freeze-out paradigm. However, a lack of evidence for a thermally produced GeV-to-TeV mass-scale Weakly Interacting Massive Particles (WIMP) in direct detection experiments and at the Large Hadron Collider (see, e.g., Refs. [30], [31], [19], [32], [46]) has motivated a theoretical effort to develop new DM

* Corresponding author.
E-mail address: j.billard@ipnl.in2p3.fr (J. Billard).

https://doi.org/10.1016/j.nuclphysb.2024.116465
Received 9 January 2024; Received in revised form 29 January 2024; Accepted 29 January 2024

Available online 6 May 2024

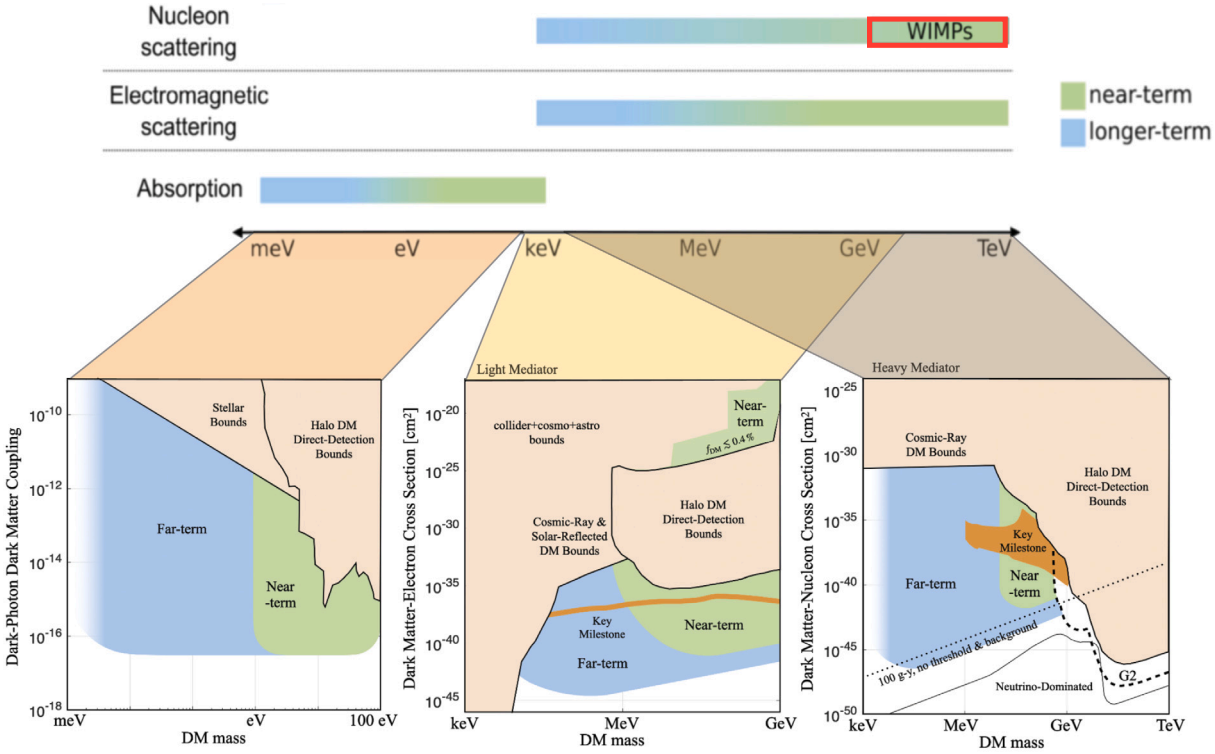

Fig. 1. Illustration of the long and near term TESSERACT targeted search sensitivities probing light dark matter particles from the meV-scale up to the proton mass considering all types of DM interactions. Figure extracted and adapted from [29].

theories that are consistent with current experimental and observational bounds. Some general properties of DM particle candidates can be established already from observational evidence and numerical simulations alone [18]. The DM particle is favoured to be *cold*, non-baryonic, should also be either absolutely stable (or extremely long lived) with only weak interactions[1] with itself or any other particles from the Standard Model. Also, the DM particle mass range can span nearly 50 orders of magnitude, from values as tiny as 10^{-21} eV (fuzzy DM) for bosons with de Broglie wavelength of the order of typical sizes of dwarf galaxies [53] up to the (reduced) Planck scale $\overline{M}_P \simeq 2 \times 10^{18}$ GeV (above which it is difficult to consider DM particles as elementary). This is as much as we can be fairly confident about the general properties of DM which, however, is only a first step towards identifying its real nature, since they can be easily satisfied by a wide range of specific particle candidates, or in fact classes of candidates. In particular, compelling models of new physics, including those of the dark sector, may naturally have mass below the weak scale. These paradigms of hidden sector DM include Hidden Valleys [57] with composite DM (whether dark mesons [48], atomic DM [45], or glueballs [43]), Asymmetric DM [44], supersymmetric hidden sector DM [41,8,49,16], strongly interacting massive particles [40], and self-interacting DM [56,37,60]. Hidden sector theories have also given rise to new approaches to deep questions, such as models for baryogenesis [23,55,20] and "neutral naturalness" [21] solutions to the hierarchy problem.

1.2. TESSERACT at the underground Modane Laboratory

The future TESSERACT (Transition Edge Sensors with Sub-eV Resolution And Cryogenic Targets) experiment aims at detecting light dark matter, from the proton mass down to a fraction of an electronvolt, via its interaction with ultra-sensitive new-generation cryogenic detectors. TESSERACT aims to be a ground-breaking experiment, representing a significant paradigm shift in relation to the current state of the art by considerably extending its light dark matter search mass range as illustrated in Fig. 1. Indeed, it aims to probe DM over 12 orders of magnitude in mass, using 1) sub-eV energy thresholds kinematically allowing to explore DM particle masses down to the (sub-)eV-scale, 2) multi-target detectors: Al_2O_3, SiO_2 GaAs, LHe, Ge and Si, to probe both nuclear (NRDM) and electronic (ERDM) recoil dark matter interactions, and 3) a technology enabling DM interactions to be identified from those arising from the radioactive and instrumental backgrounds. The combination of these last three technological features is what makes TESSERACT unique with respect to competing light dark matter experiments. Since early 2022, the French CNRS-IN2P3 laboratories IP2I, LPSC, and IJCLab are discussing with the USA-based TESSERACT collaboration in order to 1) install a dedicated cryostat for TESSERACT at the underground Modane Laboratory (LSM), and 2) include the French semiconductor germanium bolometer

[1] Here weak may stand for the familiar weak force, or instead some other (sub)weak force defined by some non-negligible coupling to the Standard Model (SM) particles.

technology (Sec. 2.5) to the initial TESSERACT science program including the SPICE (Sec. 2.3) and HeRALD (Sec. 2.4) detector technologies. The collaboration envisions to have two similar cryostats so as to allow for the operation of all three technologies, and allow some underground optimization of the detectors in one cryostat while still performing DM searches simultaneously in the second one.

The project planning phase aims to produce a fully defined experimental concept and project by the end of 2025 to achieve first competitive ultra-light DM searches starting in 2026.

2. TESSERACT detector technologies

The detection of sub-eV energy depositions from nuclear recoils with $\leq$ 50 MeV DM and electronic recoils for $\leq$ 1 MeV DM with $\geq$ 100 g.yr exposure combined with background rejection capabilities completely drives the experiment design. The proposed addition of the French semiconducting bolometer technology, based on the recent developments performed by the EDELWEISS [34] and RICOCHET [12,54,13] collaborations, will complement the initial SPICE (Sub-eV Polar Interactions Cryogenic Experiment) and HeRALD (Helium Roton Apparatus for Light Dark Matter) ones currently developed by the US collaborators. Indeed, all together, these detector technologies will be sensitive to both nuclear recoil interacting DM (NRDM) and electron recoil interacting DM (ERDM), with particle identification capabilities for background discrimination. The total mass for each target type will be between 10 g and 1 kg (depending on the target and R&D progress).

2.1. Athermal phonon Transition Edge Sensors

Athermal phonons produced directly via particle interaction, or indirectly via photon or ^{4}He atom absorption, anharmonically decay to lower-frequency phonons in the bulk of the crystal. Since this decay rate scales with the phonon energy as E^5 [58], these bulk thermalization processes turn off around $\mathcal{O}$(10 K), and the low-energy phonons begin to free stream ballistically. If the scattering surface is instrumented with superconducting phonon sensor arrays and a phonon has energy $\geq$ 4 K, it can annihilate a Cooper pair within the superconducting Al collection fins, transferring on average about 50% of its energy into kinetic and potential energy of the resulting quasi-particles. These quasi-particles subsequently diffuse within the Al film until they encounter a trapping site in the Al and are lost, or they are transmitted into the small-volume TES attached to the edge of the fins, where they thermalize their remaining energy for measurement [61].

It has been shown that the baseline energy resolution, or equivalently the energy sensitivity, of the athermal phonon detector scales as [52]:

$$\sigma_E \propto V_{\rm det}^{1/2} T_c^3. \tag{1}$$

Equation (1) illuminates the design changes required to increase sensitivity; the size of the detector must be decreased to cm^3 scale from the 100 cm^3 traditionally used by SuperCDMS [2] and EDELWEISS [10] for higher mass DM. Additionally, the critical temperature T_c must be lowered from the 40-60 mK range currently used in SuperCDMS to ideally 15-20 mK.

The TESSERACT collaboration has recently successfully demonstrated the sensitivity to detect individual optical photons with wavelengths of 405 and 450 nm. These results were obtained with a detector prototype consisting of a 1 cm^2 $\times$ 1 mm Si crystal with 1% TES surface coverage and a T_c of 50 mK. Despite its 50 mK critical temperature, this detector achieved an unprecedented baseline energy resolution of 273 meV (RMS) which could be further improved by about ten fold in lowering T_c to the targeted 15-20 mK temperatures. Using Eq. (1), one can derive that a 1 cm^3 Ge (5.35 g) or Si (2.33 g) detector should achieve sub-eV energy thresholds using optimized TES based athermal phonon sensors as currently being developed by the TESSERACT collaboration.

2.2. Low-energy excess

In recent years, as cryogenic detector experiments successfully lowered their energy threshold below $\mathcal{O}$(100) eV, a strong and yet-to-be-explained low-energy excess (LEE) background component has been observed [33]. Its level, observed in all low-threshold cryogenic experiments such as EDELWEISS [35,36], CRESST [6], RICOCHET [17], NuCLEUS [4], and SuperCDMS [3] is between 10^6 and 10^8 evt/kg/keV/day at 100 eV recoil energy, hence several orders of magnitude larger than the expected radiogenic backgrounds. This low-energy excess represents a tremendous threat to many ongoing and upcoming low-threshold cryogenic DM experiments as it may very well overwhelm the putative targeted signals and dramatically limit their search sensitivities. Among some of the general properties of this excess (see [33] for a detailed review), the EDELWEISS/RICOCHET collaborations have observed that these excess backgrounds do not ionize, hence their name “Heat-Only” (HO). As of today, the most likely hypothesis regarding this background origin is that it is either due to stress induced microfractures in the target crystal or at its interface with the phonon sensors. This suggests two important ways forward 1) find the origin of this background in order to suppress it, and 2) next generation of low-threshold cryogenic experiments must develop particle identification and/or active HO rejection techniques to achieve their expected DM sensitivities. Both strategies are being investigated by the TESSERACT collaboration.

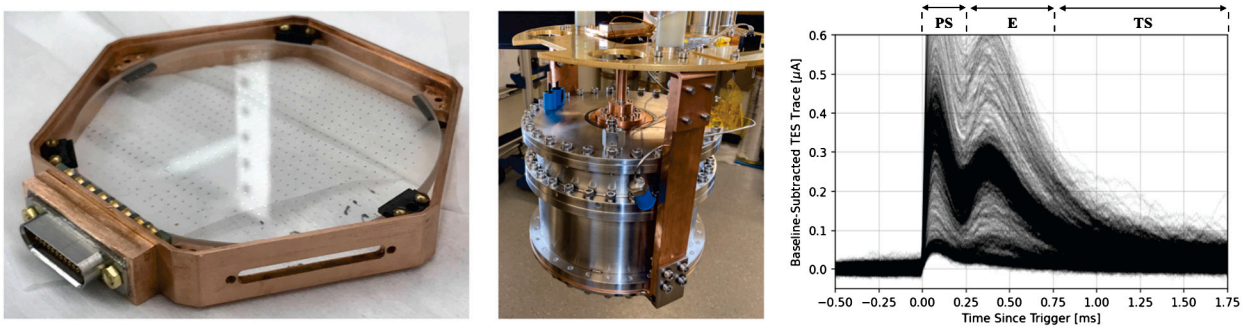

Fig. 2. Left: Photo of a first ∼10 g Al_2O_3 prototype detector from the SPICE technology. **Middle:** Photo of the HERALD v0.1 detector mounted at the mixing chamber stage of a dilution cryostat at UMass Ahmerst. **Right:** Waveforms obtained with HERALD v0.1 exposed to an ^{55}Fe source. Prompt scintillation "PS", then evaporation "E", then triplet-dominated scintillation "TS" time windows are visible. The X-ray calibration features at 5.9 and 1.5 keV are visible as denser bands (with evaporation amplitudes at $\sim 0.27\mu$A and $\sim 0.08\mu$A). Figure taken from [7].

2.3. SPICE

2.3.1. SPICE: Al_2O_3 and SiO_2 detectors

Since the vibrational energy scale in crystals is $\mathcal{O}(100)$ meV, for DM particle masses $m_{\rm DM} \leq \mathcal{O}$ (30 MeV), we can't use the simplifying approximation that the nucleus is free. Instead, we must think about the DM scattering coherently with the entire crystal producing a single phonon [38,47,39]. The kinematics of optical phonon production are favourable; due to their gapped nature, all of the kinetic energy of the DM can potentially be used for phonon creation. Additionally, since optical phonons modulate the electric dipole in polar crystals, they have strong couplings to infrared photons, and thus by extension, to all DM models that interact through a kinematically mixed dark photon.

To maximize sensitivity to these electromagnetically coupled DM models SPICE aims at developing an array of 1 cm^3 Al_2O_3 and SiO_2 detectors, instrumented on one face with athermal phonon sensors as presented in Sec. 2.1 with eV-scale energy thresholds and lower. The primary goal for these polar crystal detectors is to search for single optical phonons produced by electromagnetically interacting DM via scattering (3 keV $\leq m_{\rm DM} \leq$ 1 MeV) and via absorption (100 meV $\leq m_{\rm DM} \leq$ 1 eV). Backgrounds that directly interact with a TES/athermal phonon sensor, like stress-induced microfracture events within the athermal phonon sensor itself, are expected to be distinguishable in multiple ways. First, the athermal phonon collection time, $\tau_{\rm collect}$, is purposefully designed to be two times larger than $\tau_{\rm sensor}$. As such, events that deposit all of their energy within the TES can be distinguished from crystal interactions. Second, we can instrument each pixel with 2 separately read-out phonon sensor arrays; crystal events deposit energy nearly equally in the two arrays due to the low sensor coverage factor, while background events that interact with a single sensor would be trivially separable. Fig. 2 (left panel) shows a picture of a first $\sim$ 10 g Al_2O_3 prototype detector currently being tested by the TESSERACT collaboration.

2.3.2. SPICE: GaAs scintillation detector

Due to its small bandgap (1.52 eV), GaAs is ideally suited to search for inelastic ERs from electromagnetically coupled DM that is scattered ($m_{\rm DM} \geq$ 1 MeV) or absorbed ($m_{\rm DM} \geq$ 1.5 eV). In our detector concept, each 1 cm^3 GaAs detector is instrumented with athermal phonon sensors on its surface, and inside an optical cavity with a 1 cm^2 × 1 mm thick instrumented Ge crystal that serves as an infrared photon collector. Due to its world-leading 60% quantum efficiency for a cryogenic scintillator [24], on average nearly 12% of the total ER energy ends up in photon energy, a large fraction of which will be absorbed and sensed by the photon sensor. Requiring a coincidence of signals to differentiate signal from backgrounds is standard practice for high-mass DM searches; in particular our setup certainly builds upon the design strategies of CRESST [1]. However, there are 2 significant differences. First, GaAs has a scintillation yield of about 125 ph/keV which is ten times larger than the one of $CaWO_4$ [24]. Secondly, GaAs has similar bandgaps as Ge and Si crystals and is therefore focused on finding an electronic recoil signal in the presence of lower yield backgrounds, including zero yield backgrounds (like micro-fractures). Considering the TES based athermal phonon sensor performance described in Sec. 2.1 and the GaAs light yield, we expect to reject low-energy excess events down the eV-scale (single photon) recoil energy and extend ER/NR discrimination down to few tens of electronvolt hence allowing additional promising NRDM sensitivity that will be complementary with the semiconducting targets.

2.4. HERALD

While a strong motivation for a ^{4}He target material is the low nuclear mass, superfluid ^{4}He also has several material properties which aid in the readout of nuclear recoils. The first of these properties is the long lifetime and propagation distance of the phonon (and phonon-like 'roton') excitations. The second relevant material property is the low binding energy of ^{4}He atoms at the liquid/vacuum interface. The atomic binding energy is so low (0.62 meV) that much of the phonon/roton population lies above this energy, such that a single signal phonon can individually eject a single ^{4}He atom into the vacuum. This athermal 1-to-1 process is termed 'quantum evaporation'. Several theoretical descriptions of this process have been given [26,27,22], and are in general qualitative

agreement, predicting evaporation probabilities (per phonon incidence at the interface) of some 10s of percent. Experiments have shown broad consistency with theoretical prediction [28]. A sensor or sensor array in the vacuum region then receives a burst of ejected ^{4}He atoms as the primary signal, and these atoms are sensed via their van der Waals binding energy to the sensor surface (∼10 meV per adsorbed atom). The third relevant property is the helium superfluidity. As it is a liquid target, there should be no mechanical micro-fractures-like events within the helium itself contributing to "Heat-Only" (HO) backgrounds. Vibrational coupling is suppressed between the vessel walls and the superfluid helium, since objects move through pure superfluid helium without viscosity. Scattering events within the helium will produce rotons and phonons, yielding evaporated helium atoms to be detected on multiple athermal phonon pixels suspended above the liquid. Therefore, requiring coincidence between multiple pixels should drastically reduce HO backgrounds, even if individual pixels have HO events within them. Finally, superfluid helium is a very bright scintillator, with about 33% of ER energy going into prompt scintillation light. The NR light yield, while nonlinear with energy, is also very high: at energies measured so far we find a Lindhard quenching factor of 40%, corresponding to 13% of NR energy going into prompt scintillation. The scintillation signal will be another handle on discriminating ER events, NR events, and instrumental backgrounds for higher DM masses.

Early 2023, the HeRALD team successfully built and tested their first detector prototype [7]. Fig. 2 middle shows a picture of the HERALD v0.1 prototype detector equipped with a Cs-based superfluid He film stopper and a photon/^{4}He detector, instrumented with athermal phonon TES, facing a 2.75 cm high and 6 cm diameter liquid ^{4}He cell corresponding to about a total He target mass of 10 g. Right panel of Fig. 2 shows some first data from the HERALD v0.1 detector prototype exposed to a ^{55}Fe source emitting 5.9 keV X-rays accompanied with 1.5 keV X-rays from aluminum fluorescence. From these first data set, one can clearly appreciate the detection of the prompt scintillation signal "PS" followed by the one from the ^{4}He quantum evaporation "E", eventually followed by the triplet scintillation "TS". For these data, the detection threshold for energy in the ^{4}He quasiparticle system is approximately 145 eV, which already corresponds to a very promising light dark matter mass sensitivity $m_{\rm DM} \geq 220$ MeV/c^2 [7].

2.5. Cryogenic semiconducting bolometers

The EDELWEISS [10] and SuperCDMS [2] experiments have pioneered the use of cryogenic semiconductor crystals (Ge and Si) to search for DM particles. In this section we detail the proposed semiconducting bolometer detector technology contribution for the TESSERACT experiment at LSM. Our plan is to focus on both ERDM and NRDM searches with optimized semiconducting cryogenic detectors, which builds upon the legacy of the former EDELWEISS [2] experiment and today's RICOCHET [13] and CRYOSEL programs. For now the focus is on using Ge target material, given its excellent performance and acquired expertise, but complimentary targets such as Si and diamond will be investigated at later stages.

Following a particle's interaction in the detector medium, the induced recoil will release its energy by creating both phonons (heat) and charge carriers (ionization). To first order,[2] the different measurable energy quantities are intertwined as follows:

$$\begin{aligned} E_{\rm ion} &= Q(E_R)E_R \ , \\ E_{\rm NTL} &= E_{\rm ion}\frac{V}{\epsilon} \ , \\ E_{\rm heat} &= E_R + E_{\rm NTL} = E_R\left[1 + Q(E_R)\frac{V}{\epsilon}\right] \end{aligned} \tag{2}$$

where V is the voltage bias and ϵ is the average energy required for an electron recoil to produce an electron-hole pair. $E_{\rm heat}$ and $E_{\rm ion}$ stand for the heat and ionisation energies, respectively. $E_{\rm NTL}$ is the additional Neganov-Trofimov-Luke heat energy produced by drifting the charge carriers across the crystal [50,51]. The quenching factor $Q(E_R)$ is by definition equal to 1 for ER, between 0 and 0.3 for NR below 20 keV [14], and equal to 0 for "Heat-Only" backgrounds. It is worth highlighting that, in addition to the event-by-event discrimination, the simultaneous heat and ionisation energy measurements at V $\neq$ 0 also provides a direct measurement of the true nuclear recoil energy, hence avoiding any assumptions on the ionisation yield. Following Eq. (2), two operating modes can be considered.

Low-voltage mode: By operating the detector at low enough bias voltages (≤4 V), such that $E_{\rm NTL} < E_R$ for nuclear recoils, the simultaneous measurement of heat and ionisation provides an event-by-event identification of the recoil type, hence allowing a highly efficient rejection of the dominant low-energy excess and gamma backgrounds. Residual gamma- and surface beta-backgrounds are further removed using active surface rejection, based on either veto electrodes or charge asymmetry, of the FID (Fully Interdigitised Design) from the EDELWEISS [34] experiments.

High-voltage mode: By operating the detector at high voltage biases (≥100 V), the cryogenic calorimeter is effectively turned into a charge amplifier of mean gain $(1 + Q(E_R)\frac{V}{\epsilon})$. As $E_{\rm heat} \simeq E_{\rm ion}$, event-by-event discrimination is no longer possible and an ionization yield model has to be assumed to convert the total heat energy into a nuclear recoil energy equivalent. This operation mode is highly beneficial to any DM searches looking for interactions with electrons instead of nuclei. First, the total phonon signal is amplified by a factor $(1 + \frac{V}{\epsilon})$, while the HO background is not. Electron recoil signal should then appear as discrete peaks corresponding to $E_{NTL} = N|eV|$ where N is the number of electron-hole pairs, e is the electron charge. For bias voltages such that eV is significantly larger

[2] We neglect here the phonon energy loss due to Frenkel defects and to charge trapping.

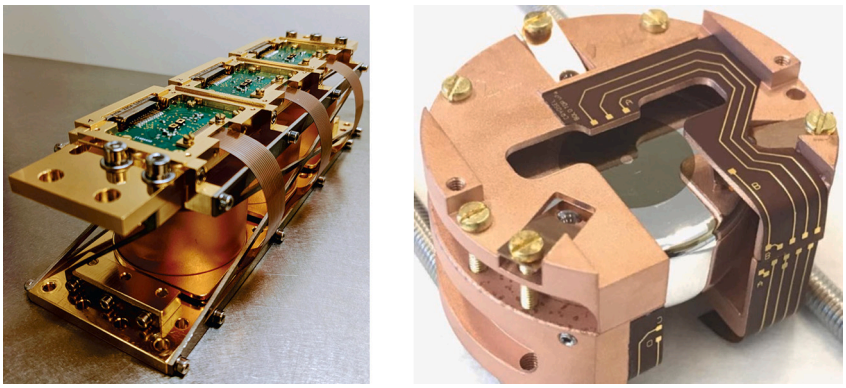

Fig. 3. Left: Photo of a MiniCryoCube assembly, hosting the detectors RED127, RED167, and RED237 (from left to right), with its two stages at 10 mK hosting the three detectors, and at 1 K hosting the HEMT-based electronics. **Right:** Picture of the first CRYOSEL detector prototype.

than the phonon sensor resolution, ERDM signals should form comb-like structure, differentiable from a smooth background of HO events.

2.5.1. NRDM searches with low-voltage semiconducting detectors

The goal of the "low voltage" semiconducting cryogenic bolometer program is to achieve unprecedented NRDM sensitivities down to 50 MeV DM mass with highly efficient particle identification and background rejection capabilities, against bulk and surface backgrounds, and against the overwhelming "Heat-Only" excess. To achieve this scientific goal, and based upon the charge and phonon readout developments from RICOCHET and the athermal TES from TESSERACT (see Sec. 2.1), we propose to develop 1 cm^3 crystal targets with ultimate 3 eV_{ee} and 100 meV ionization and phonon baseline energy resolutions (RMS), respectively.

These planned developments build upon the ongoing effort and expertise from the RICOCHET collaboration [12] currently developing the next generation of "low-voltage" Ge cryogenic detectors, called CryoCube, designed to reach $\sigma_{\text{ion}} = 20$ eV_{ee} and $\sigma_{\text{ph}} = 20$ eV baseline energy resolution (RMS) in ionization and phonon energies, respectively, with a total payload of 1 kg of Ge target material [54]. Fig. 3 (left panel) is a photo of a sub-array of the CryoCube, called MiniCryoCube, which can host up to three 42 g Ge crystal detectors equipped with an NTD (Neutron Transmutation Dopped) heat sensor and aluminum electrodes to simultaneously measure both the phonon and ionization energies following a particle interaction. The MiniCryoCube is made of two stages, a 10 mK stage hosting the three detectors and a 1 K stage hosting the front-end HEMT-based electronics for the ionization readout.[3] The RICOCHET collaboration has already demonstrated a first 30 eV_{ee}-scale baseline ionization resolution (RMS), which is about 7 and 11 times lower than its EDELWEISS [10] and SuperCDMS [2] predecessors, and is now testing its newly designed room temperature electronics that allows for a dual measurement of phonon and ionization energies [15]. First dual readout performance were about 44 eV_{ee} and 60 eV baseline resolutions (RMS) for the ionization and phonon energies, respectively, leading to a factor of about 10 reduction in the particle identification thresholds compared to past EDLEWEISS-III performance [34].

Reaching the targeted resolutions listed above in the context of TESSERACT will require to improve further on these already achieved performance. Regarding the ionization channel, optimized electrode and crystal holder designs will be developed in order to achieve a detector capacitance of 1 pF with negligible parasitic capacitance. Our HEMT-based preamplifier model suggests that with a 2 pF total capacitance (detector + HEMT) we could achieve single-electron charge resolution readout [42]. On the phonon resolution side, we plan to switch from the currently used NTD to the more sensitive athermal phonon TES sensors discussed in Sec. 2.1 from the TESSERACT collaboration. Additionally, in depth studies are ongoing to reduce the TES film induced stress in order to potentially dramatically reduce the overwhelming non-ionising low-energy excess.

2.5.2. ERDM searches with high-voltage semiconducting detectors

The scientific objective of the "high voltage" semiconducting cryogenic bolometer program is to search for sub-MeV dark matter particles with electronic recoils (ERDM). The goal of this development is to achieve single electron-hole pair sensitivity with an active heat-only veto and low leakage currents. Within this context a new detector design, called CRYOSEL, is currently being developed.

In this detector design the charge electrode readout is replaced by a very sensitive athermal phonon sensor, detecting the large flux of phonons emitted via the NTL amplification process when charges drift through a small, very high electric field region. This specific field configuration is achieved by using the phonon sensor itself as a point-contact like electrode, as shown in Fig. 3 (right panel). An NbSi layer deposited on the crystal surface is patterned to a 10 μm circular line having a diameter of 2 to 5 mm. The NbSi film can operate either as a TES or in a proposed innovative regime called SSED (Superconducting Single Electron Device) well below its critical temperature. At high charge-collecting voltage the SSED is expected to trigger on single electron-hole events and tag the presence of charge. While phonons emitted by HO events may be expected to be distributed uniformly over the entire crystal volume,

[3] The High Electron Mobility Transistors (HEMT) used in our work are developed by the Center for Nanoscience and Nanotechnology (C2N) and commercialized by CryoHEMT [25].

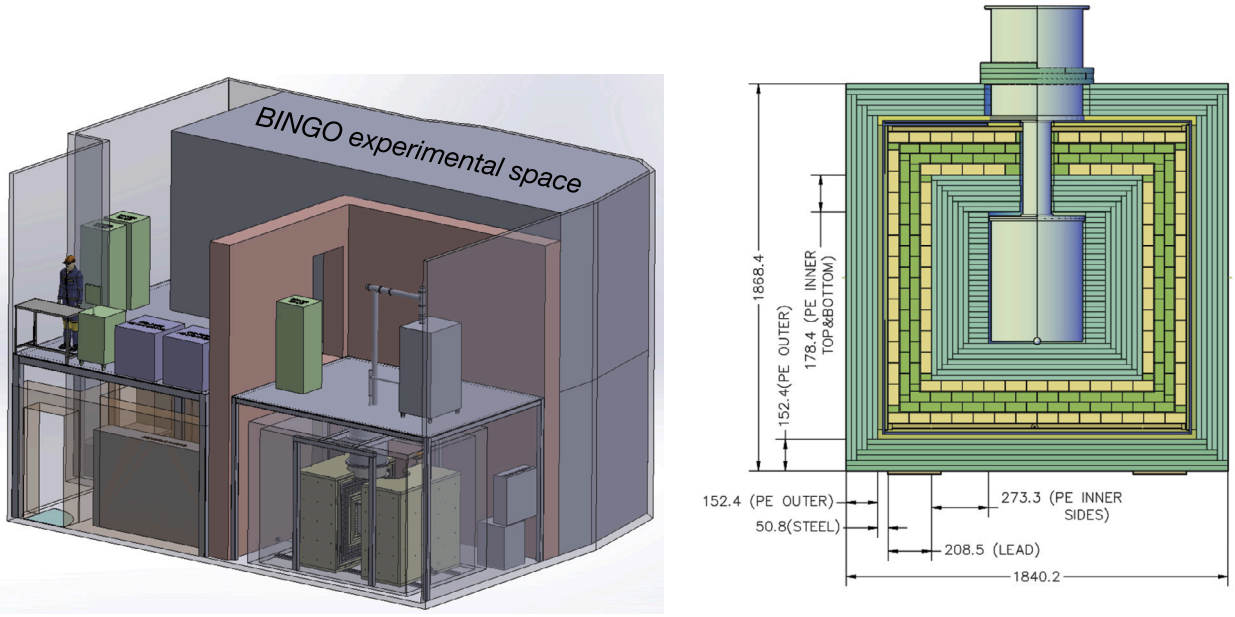

Fig. 4. Left: Proposed preliminary layout of the TESSERACT experiment at LSM - Phase I sharing the former EDELWEISS-III experimental space [10] with the BINGO $0\nu\beta\beta$ experiment [9]. **Right:** TESSERACT shielding with dimensions surrounding the central cryostat. We have, from outside to inside, a layer of PE, a stainless steel enclosure, lead bricks, another layer of PE, and then the cryostat. All measurements are in mm.

nearly all NTL phonons are emitted in a few mm^3 zone located under the NbSi microwire phonon sensor. In these conditions a high suppression factor of the HO event rate is expected. The SSED design will be optimized to trigger on single-charge events but is not expected to read the charge signal with a high resolution. A high-resolution measurement will be provided by a NTD-Ge thermistor or an athermal phonon TES sensor. A 20 eV phonon resolution and a bias of 200 V is sufficient to provide a <10% resolution on the peaks due to the detection of discrete number of electron-hole pairs. ERDM signals should thus correspond to discrete Gaussian peaks over the smooth HO background spectrum, strongly suppressed by the SSED rejection efficiency.

The CRYOSEL project has already achieved its primary goal of establishing that this original method to tag charges using NTL phonons does indeed work down to 1 keV. The CRYOSEL developments are now in the process of reducing the thresholds of the SSED and of increasing the voltage bias up to 200 V. This intense program should rapidly provide the two orders of magnitude improvement on the energy threshold needed to obtain discrimination at the single-electron level. In addition, the ability to compare charge, thermal and athermal signals in coincidence will soon provide information on the nature and origin of the HO background that will be very useful in optimizing future low- and high-voltage semiconducting detector designs.

3. Experimental apparatus at the Modane Underground Laboratory

The Modane Underground Laboratory (LSM) is a French national lab dedicated to the development of the astroparticle physics programme. Being protected from cosmic rays, it provides the low background conditions necessary for experiments dealing with rare or exotic interactions. It has been proven to be an ideal site for cryogenic searches for DM and for neutrinoless double-beta decay, as attested by the success of the EDELWEISS [34] and CUPID-Mo [11] programs.

The mean rock thickness of 1700 m (about 4800 m water equivalent) reduces the muon flux down to about 5 muons/m^2/d [59], which is more than 10^6 times smaller than at the surface. To further protect the TESSERACT detectors, this time from the surrounding rock radioactivity, they will be protected by passive shielding layers (see Sec. 3.1). Fig. 4 (left panel) shows the preliminary version of the planned layout of the Phase-1 cryostat (see Sec. 1.2) of the TESSERACT experiment at LSM. The experimental setup, consisting of the cryogenics system, shielding, electronics, data acquisition along with the specialized ISO-6 clean room will be located in the previous EDELWEISS location. Utilities for the cryogenic system and radon suppression will be located on the mezzanine of the above mentioned area.

3.1. Shielding design

The shielding for TESSERACT is being designed based on early Monte Carlo simulations. They infer the acceptable contamination levels of the shielding materials along with their size. A sketch of the experimental set-up along with the shielding scheme is shown in Fig. 4 (right panel).

The overall design of the TESSERACT shielding follows well-established techniques for reducing environmental backgrounds, using layers of hydrogenous material for neutron moderation and high-Z material to reduce the gamma flux. The final layer of shielding, closest to the detectors, must be of the highest radiopurity material. The outermost layer of the TESSERACT shield is

composed of 15 cm of high density polyethylene (HDPE), which reduces radiogenic neutrons produced in the cavern walls. This first line of defense is called the outer neutron shield. The next layer inwards is a 20 cm-thick gamma shield made of lead which reduces the accompanying external gamma flux. This is followed by an additional layer of 27 cm polyethylene between the lead and the titanium outer vacuum can of the cryostat. This inner neutron shield attenuates any secondary neutrons from spallation, as well as neutrons and gammas emitted by trace internal radioactivity in either the cryostat or the lead. The "self-shielding" capability of the shield design, where each layer reduces the background flux from the outward layers, is a critical design feature. This enables a design in which only the innermost materials must be of exceedingly high purity, while the outer shielding layers can have looser purity restrictions, reducing costs for screening and assay.

Protection from prompt radon gammas and prevention of radon daughter contamination over time necessitates a 5 cm-thick radon barrier layer outside the lead to maintain a nitrogen atmosphere within the shield interstices. A radiopure mu-metal shield between the inner neutron shield and the cryostat is also required in order to reduce the Earth's magnetic field at the detectors. Indeed, the phonon readout of TESSERACT detectors is based on SQUID amplifiers which performance (in particular their noise) is impacted by external magnetic fields. The required reduction of the external magnetic fields to a value close to $\sim 1\ \mu$T (at least a factor 50 below the Earth's value) will be achieved with a mu-metal cylinder of ~ 1 mm thickness around the external can of the cryostat.

3.2. Background budget

To achieve world-leading light dark matter sensitivities with TESSERACT, it is of the utmost importance to reach the lowest radioactive background levels. The overall targeted background levels of TESSERACT, before any detector rejection cuts, is in the order of 1 evt/kg/keV/day for the gammas and less than 10^{-3} evt/kg/keV/day for the neutrons.

Initial simulations performed by TESSERACT are based on the rock composition and density of the Homestake formation. A statistic of 10^{10} external γ-rays from ^{238}U and ^{232}Th chains and about 10^{9} neutron events from (α,n) and spontaneous fission in cavern walls were simulated. Internal backgrounds of the shielding material are modeled using measured radioactive activities in titanium, stainless steel, copper, and polyethylene as published by SuperCDMS, EDELWEISS, LZ and other experiments. Extensive simulations of the entire TESSERACT installation as planned for LSM will be done in order to finalize the selection of the construction materials and optimize the passive shielding design, satisfy the background requirements, and set limits on the amount of cosmic ray exposure. It is worth mentioning that the TESSERACT experimental setup at Modane will also be equipped with a dual Broad Energy Ge (BEGe) detector from Mirion and an XIA UltraLo-1800 for screening and assay of material radiopurity and surfaces, respectively.

If a lower background budget is required for TESSERACT, we would pay attention to it during the shield design study considering additional gamma shielding to reduce potential gaps, and replacing the highest contributors from the facility (TFA lead shield and OVC) with lower activity materials (lower activity lead for the shield for instance). For the OVC, TESSERACT is indeed considering clean radiopure titanium material from LZ experiment. Lastly, specifically designed cryogenic detectors acting as active veto, as planned by the BINGO [9] and NuCLEUS [5] experiments for example, could be used to further reduce the TESSERACT background levels if needed.

4. Conclusions

The future TESSERACT experiment aims at extending the Dark Matter mass search window from meV-to-GeV with ultra low-threshold cryogenic detectors with multiple targets, particle identification and LEE rejection capabilities. Here we discussed the proposal to host the TESSERACT experiment at the Modane Underground Laboratory and include a third cryogenic detector technology to the initial payload. Combined with the US-based SPICE and HeRALD technologies, the TESSERACT at LSM experiment will then allow to probe DM candidates over 12 orders of magnitude in mass, using ERDM and NRDM signatures with 100 meV-scale energy threshold, multiple target materials, and state of the art background levels thanks to an optimal shielding design and radiopure material selection. As such, the future TESSERACT experiment will be uniquely positioned to lead the sub-GeV dark matter search program in the coming years.

CRediT authorship contribution statement

Julien Billard is the presenter to the Nobel Symposium on Dark Matter, the main contributor to the text of theses proceedings, and the French PI of the proposed TESSERACT@LSM future experiment. Jules Gascon, Stefanos Marnieros and Silvia Scorza each participated to the writing of these proceedings and the design of this proposed experiment as French Co-PIs.

Declaration of competing interest

The authors declare the following financial interests/personal relationships which may be considered as potential competing interests: Julien Billard reports financial support was provided by European Research Council. Jules Gascon reports a relationship with French National Research Agency that includes: funding grants. If there are other authors, they declare that they have no known competing financial interests or personal relationships that could have appeared to influence the work reported in this paper.

Data availability

Data will be made available on request.

Acknowledgements

Some of the work presented here received funding from the European Research Council (ERC) under the European Union's Horizon 2020 research and innovation program under Grant Agreement ERC-StG-CENNS 803079, the French National Research Agency (ANR) within the project ANR-21-CE31-0004 (CRYOSEL), and the LABEX Lyon Institute of Origins (ANR-10-LABX-0066) of the Université de Lyon, within the Plan France2030.

References

[1] A.H. Abdelhameed, et al., First results from the CRESST-III low-mass dark matter program, Phys. Rev. D 100 (10) (2019) 102002, https://doi.org/10.1103/PhysRevD.100.102002.
[2] R. Agnese, et al., Results from the super cryogenic dark matter search experiment at Soudan, Phys. Rev. Lett. 120 (6) (2018) 061802, https://doi.org/10.1103/PhysRevLett.120.061802.
[3] I. Alkhatib, et al., Light dark matter search with a high-resolution athermal phonon detector operated above ground, Phys. Rev. Lett. 127 (2021) 061801, https://doi.org/10.1103/PhysRevLett.127.061801.
[4] G. Angloher, et al., Results on MeV-scale dark matter from a gram-scale cryogenic calorimeter operated above ground, Eur. Phys. J. C 77 (9) (2017) 637, https://doi.org/10.1140/epjc/s10052-017-5223-9.
[5] G. Angloher, et al., Exploring CEνNS with NUCLEUS at the Chooz nuclear power plant, Eur. Phys. J. C 79 (12) (2019) 1018, https://doi.org/10.1140/epjc/s10052-019-7454-4.
[6] G. Angloher, et al., Results on sub-GeV dark matter from a 10 eV threshold CRESST-III silicon detector, Phys. Rev. D 107 (12) (2023) 122003, https://doi.org/10.1103/PhysRevD.107.122003.
[7] R. Anthony-Petersen, et al., Applying superfluid helium to light dark matter searches: demonstration of the HeRALD detector concept, arXiv:2307.11877 [physics.ins-det], 7 2023.
[8] Nima Arkani-Hamed, Neal Weiner, LHC signals for a SuperUnified theory of dark matter, J. High Energy Phys. 2008 (12) (dec 2008) 104, https://doi.org/10.1088/1126-6708/2008/12/104.
[9] A. Armatol, et al., First cryogenic tests on BINGO innovations, in: 32nd Rencontres de Blois on Particle Physics and Cosmology, 4 2022.
[10] E. Armengaud, et al., Performance of the EDELWEISS-III experiment for direct dark matter searches, J. Instrum. 12 (08) (2017) P08010, https://doi.org/10.1088/1748-0221/12/08/P08010.
[11] E. Armengaud, et al., New limit for neutrinoless double-beta decay of ^{100}Mo from the CUPID-Mo experiment, Phys. Rev. Lett. 126 (18) (2021) 181802, https://doi.org/10.1103/PhysRevLett.126.181802.
[12] C. Augier, et al., Fast neutron background characterization of the future Ricochet experiment at the ILL research nuclear reactor, Eur. Phys. J. C 83 (1) (2023) 20, https://doi.org/10.1140/epjc/s10052-022-11150-x.
[13] C. Augier, et al., First Demonstration of 30 eVee Ionization Energy Resolution with Ricochet Germanium Cryogenic Bolometers, 5 2023.
[14] D. Barker, W.Z. Wei, D.M. Mei, C. Zhang, Ionization efficiency study for low energy nuclear recoils in germanium, Astropart. Phys. 48 (8) (2013), https://doi.org/10.1016/j.astropartphys.2013.06.010.
[15] G. Baulieu, et al., HEMT-based 1 K front-end electronics for the heat and ionization Ge CryoCube of the future ricochet CEνNS experiment, J. Low Temp. Phys. 209 (3–4) (2022) 570–580, https://doi.org/10.1007/s10909-022-02896-5.
[16] Matthew Baumgart, Clifford Cheung, Joshua T. Ruderman, Lian-Tao Wang, Itay Yavin, Non-abelian dark sectors and their collider signatures, J. High Energy Phys. 2009 (04) (apr 2009) 014, https://doi.org/10.1088/1126-6708/2009/04/014.
[17] Julien Billard, Searching for Dark Matter and New Physics in the Neutrino sector with Cryogenic detectors, Habilitation à diriger des recherches, Université Claude Bernard Lyon 1, January 2021, https://theses.hal.science/tel-03259707.
[18] Julien Billard, et al., Direct detection of dark matter—APPEC committee report, Rep. Prog. Phys. 85 (5) (2022) 056201, https://doi.org/10.1088/1361-6633/ac5754.
[19] Antonio Boveia, Caterina Doglioni, Dark matter searches at colliders, (ISSN 0163-8998) 68 (2018) 429–459, https://doi.org/10.1146/annurev-nucl-101917-021008.
[20] Matthew R. Buckley, Lisa Randall, Xogenesis, J. High Energy Phys. 2011 (9) (sep 2011), https://doi.org/10.1007/jhep09(2011)009.
[21] Z. Chacko, Hock-Seng Goh, Roni Harnik, Natural electroweak breaking from a mirror symmetry, Phys. Rev. Lett. 96 (23) (jun 2006), https://doi.org/10.1103/physrevlett.96.231802.
[22] F. Dalfovo, M. Guilleumas, A. Lastri, L. Pitaevskii, S. Stringari, Quantum evaporation from superfluid helium at normal incidence, J. Phys. Condens. Matter 9 (24) (jun 1997) L369, https://doi.org/10.1088/0953-8984/9/24/004.
[23] Hooman Davoudiasl, David E. Morrissey, Kris Sigurdson, Sean Tulin, Unified origin for baryonic visible matter and antibaryonic dark matter, Phys. Rev. Lett. 105 (21) (nov 2010), https://doi.org/10.1103/physrevlett.105.211304.
[24] S. Derenzo, E. Bourret, S. Hanrahan, G. Bizarri, Cryogenic scintillation properties of n-type GaAs for the direct detection of MeV/c^2 dark matter, J. Appl. Phys. 123 (11) (2018) 114501, https://doi.org/10.1063/1.5018343.
[25] Quan Dong, Ying-Xin Liang, D. Ferry, Antonella Cavanna, U. Gennser, L. Couraud, Yong Jin, Ultra-low noise high electron mobility transistors for high-impedance and low-frequency deep cryogenic readout electronics, Appl. Phys. Lett. 105 (2014) 013504, https://doi.org/10.1063/1.4887368.
[26] P.M. Echenique, J.B. Pendry, Reflectivity of liquid ^{4}He surfaces to ^{4}He atoms, Phys. Rev. Lett. 37 (Aug 1976) 561–563, https://doi.org/10.1103/PhysRevLett.37.561.
[27] D.O. Edwards, P.P. Fatouros, Theory of atomic scattering at the free surface of liquid ^{4}He, Phys. Rev. B 17 (Mar 1978) 2147–2159, https://doi.org/10.1103/PhysRevB.17.2147.
[28] C. Enss, S.R. Bandler, R.E. Lanou, H.J. Maris, T. More, F.S. Porter, G.M. Seidel, Quantum evaporation of 4He: angular dependence and efficiency, Physica B, Condens. Matter (ISSN 0921-4526) 194–196 (1994) 515–516, https://doi.org/10.1016/0921-4526(94)90587-8.
[29] Rouven Essig, et al., Snowmass2021 Cosmic Frontier: the landscape of low-threshold dark matter direct detection in the next decade, in: Snowmass 2021, 3 2022.
[30] D.S. Akerib, et al., Results from a search for dark matter in the complete lux exposure, Phys. Rev. Lett. 118 (Jan 2017) 021303, https://doi.org/10.1103/PhysRevLett.118.021303.
[31] E. Aprile, et al., Dark matter search results from a one ton-year exposure of xenon1t, Phys. Rev. Lett. 121 (Sep 2018) 111302, https://doi.org/10.1103/PhysRevLett.121.111302.
[32] M. Aaboud, et al., Search for new phenomena in final states with an energetic jet and large missing transverse momentum in pp collisions at $\sqrt{s} = 13$ TeV using the atlas detector, Phys. Rev. D 94 (Aug 2016) 032005, https://doi.org/10.1103/PhysRevD.94.032005.
[33] P. Adari, et al., EXCESS workshop: descriptions of rising low-energy spectra, SciPost Phys. Proc. 9 (aug 2022), https://doi.org/10.21468/scipostphysproc.9.001.
[34] E. Armengaud, et al., EDELWEISS Collaboration, Performance of the EDELWEISS-III experiment for direct dark matter searches, J. Instrum. 12 (08) (aug 2017) P08010, https://doi.org/10.1088/1748-0221/12/08/p08010.

[35] E. Armengaud, et al., EDELWEISS Collaboration, Searching for low-mass dark matter particles with a massive Ge bolometer operated above ground, Phys. Rev. D 99 (8) (apr 2019), https://doi.org/10.1103/physrevd.99.082003.
[36] Q. Arnaud, et al., EDELWEISS Collaboration, First germanium-based constraints on sub-MeV dark matter with the EDELWEISS experiment, Phys. Rev. Lett. 125 (14) (oct 2020), https://doi.org/10.1103/physrevlett.125.141301.
[37] Jonathan L. Feng, Manoj Kaplinghat, Huitzu Tu, Hai-Bo Yu, Hidden charged dark matter, J. Cosmol. Astropart. Phys. 2009 (07) (jul 2009) 004, https://doi.org/10.1088/1475-7516/2009/07/004.
[38] Sinead Griffin, Simon Knapen, Tongyan Lin, Kathryn M. Zurek, Directional detection of light dark matter with polar materials, Phys. Rev. D 98 (11) (2018) 115034, https://doi.org/10.1103/PhysRevD.98.115034.
[39] Sinéad M. Griffin, Katherine Inzani, Tanner Trickle, Zhengkang Zhang, Kathryn M. Zurek, Multichannel direct detection of light dark matter: target comparison, Phys. Rev. D 101 (Mar 2020) 055004, https://doi.org/10.1103/PhysRevD.101.055004.
[40] Yonit Hochberg, Eric Kuflik, Tomer Volansky, Jay G. Wacker, Mechanism for thermal relic dark matter of strongly interacting massive particles, Phys. Rev. Lett. 113 (Oct 2014) 171301, https://doi.org/10.1103/PhysRevLett.113.171301.
[41] Dan Hooper, Kathryn M. Zurek, Natural supersymmetric model with MeV dark matter, Phys. Rev. D 77 (8) (apr 2008), https://doi.org/10.1103/physrevd.77.087302.
[42] A. Juillard, et al., Low-noise HEMTs for coherent elastic neutrino scattering and low-mass dark matter cryogenic semiconductor detectors, J. Low Temp. Phys. 199 (3–4) (2019) 798–806, https://doi.org/10.1007/s10909-019-02269-5.
[43] Junhai Kang, Markus A. Luty, Macroscopic strings and "quirks" at colliders, J. High Energy Phys. 2009 (11) (nov 2009) 065, https://doi.org/10.1088/1126-6708/2009/11/065.
[44] David E. Kaplan, Markus A. Luty, Kathryn M. Zurek, Asymmetric dark matter, Phys. Rev. D 79 (Jun 2009) 115016, https://doi.org/10.1103/PhysRevD.79.115016.
[45] David E. Kaplan, Gordan Z. Krnjaic, Keith R. Rehermann, Christopher M. Wells, Atomic dark matter, J. Cosmol. Astropart. Phys. 2010 (05) (may 2010) 021, https://doi.org/10.1088/1475-7516/2010/05/021.
[46] V. Khachatryan, et al., Search for disappearing tracks in proton-proton collisions at $\sqrt{s} = 8$ TeV, J. High Energy Phys. 01 (2015) 096, https://doi.org/10.1007/JHEP01(2015)096.
[47] Simon Knapen, Tongyan Lin, Matt Pyle, Kathryn M. Zurek, Detection of light dark matter with optical phonons in polar materials, Phys. Lett. B 785 (2018) 386–390, https://doi.org/10.1016/j.physletb.2018.08.064.
[48] Graham D. Kribs, Tuhin S. Roy, John Terning, Kathryn M. Zurek, Quirky composite dark matter, Phys. Rev. D 81 (9) (may 2010), https://doi.org/10.1103/physrevd.81.095001.
[49] Jason Kumar, Jonathan L. Feng, George Alverson, Pran Nath, Brent Nelson, WIMPless dark matter, in: AIP Conference Proceedings, AIP, 2010.
[50] P.N. Luke, Voltage-assisted calorimetric ionization detector, J. Appl. Phys. 64 (6858) (1988) 6858, https://doi.org/10.1063/1.341976.
[51] B.S. Neganov, V.N. Trofimov, Colorimetric method measuring ionizing radiation, Otkryt. Izobret. 146 (1985) 215.
[52] Matt Pyle, Enectali Feliciano-Figueroa, Bernard Sadoulet, Optimized Designs for Very Low Temperature Massive Calorimeters, 3 2015.
[53] Mohammadtaher Safarzadeh, David N. Spergel, Ultra-light dark matter is incompatible with the Milky Way's dwarf satellites, https://doi.org/10.3847/1538-4357/ab7db2, 6 2019.
[54] T. Salagnac, et al., Optimization and performance of the CryoCube detector for the future ricochet low-energy neutrino experiment, J. Low Temp. Phys. 211 (5–6) (2023) 398–406, https://doi.org/10.1007/s10909-023-02960-8.
[55] Jessie Shelton, Kathryn M. Zurek, Darkogenesis: a baryon asymmetry from the dark matter sector, Phys. Rev. D 82 (Dec 2010) 123512, https://doi.org/10.1103/PhysRevD.82.123512.
[56] David N. Spergel, Paul J. Steinhardt, Observational evidence for self-interacting cold dark matter, Phys. Rev. Lett. 84 (Apr 2000) 3760–3763, https://doi.org/10.1103/PhysRevLett.84.3760.
[57] Matthew J. Strassler, Kathryn M. Zurek, Echoes of a hidden valley at hadron colliders, Phys. Lett. B (ISSN 0370-2693) 651 (5) (2007) 374–379, https://doi.org/10.1016/j.physletb.2007.06.055.
[58] Shin-ichiro Tamura, Spontaneous decay rates of la phonons in quasi-isotropic solids, Phys. Rev. B 31 (Feb 1985) 2574–2577, https://doi.org/10.1103/PhysRevB.31.2574.
[59] B. Schmidt, et al., Muon-induced background in the EDELWEISS dark matter search, Astropart. Phys. 44 (apr 2013) 28–39, https://doi.org/10.1016/j.astropartphys.2013.01.014.
[60] Sean Tulin, Hai-Bo Yu, Kathryn M. Zurek, Beyond collisionless dark matter: particle physics dynamics for dark matter halo structure, Phys. Rev. D 87 (11) (jun 2013), https://doi.org/10.1103/physrevd.87.115007.
[61] J.J. Yen, B. Shank, B.A. Young, B. Cabrera, P.L. Brink, M. Cherry, J.M. Kreikebaum, R. Moffatt, P. Redl, A. Tomada, E.C. Tortorici, Measurement of quasiparticle transport in aluminum films using tungsten transition-edge sensors, Appl. Phys. Lett. (ISSN 0003-6951) 105 (16) (10 2014) 163504, https://doi.org/10.1063/1.4899130.